Foresail-1p

Digital Sun Sensor Hardware Design v5

Aalto University

Department of Electronics and Nanoengineering

Authors

Name	Worked with parts
Bruce Clayhills	**The whole document**
Marius Anger	**Hardware revision 5**

Table of Contents

1 General **4**
1.1 Scope 4
1.2 Reference Documents 4
1.3 Abbreviations and Acronyms 5
2 Sensor Design **5**
2.1 DSS General Characteristics: 6
2.2 Mechanical Cover 6
2.3 ND-Filter & Mask Design 7
2.4 Theoretical FOV 8
2.5 Theoretical accuracy 9
3 Electrical Design **9**
3.1 Microcontroller 10
3.2 S9132 Profile Sensor 11
3.3 Power Supply 11
3.4 Inrush current 12
3.5 Sensor Gain Selection 14
3.6 Environment 15
4 Software **15**
5 Calibration and Validation **15**
Appendices **17**
A. Schematics 17
B. PCB Layout 17

1 General

1.1 Scope

The purpose of this document is to present the current digital sun sensor design for Foresail-1p. This document is made for the hardware revision 5, and is mainly based on the Hamamatsu S9132 profile sensor.

The design files related to this document and version can be found on the following Github repository:
Revision 1-4: https://github.com/aaltosatellite/foresail/tree/master/dss_sunsensor
Revision 5: https://github.com/aaltosatellite/fs1p_adcs/tree/main/dss_sunsensor

1.2 Reference Documents

1. Hamamatsu S9132 Profile Sensor - datasheet: https://www.hamamatsu.com/resources/pdf/ssd/s9132_kmpd1075e.pdf
2. Texas Instrument's MSP430FR5739 datasheet: http://www.ti.com/lit/ds/symlink/msp430fr5739.pdf
3. FS1 PSD Sun Sensor Design: https://docs.google.com/document/d/1SByVZYXU1UmMgaHT1f_zqc_vpBboQWTH_l9uw-Ily4A/edit#
4. FS1 ADCS Digital Sun Sensor Software Design Document
5. FS1 ADCS Digital Sun Sensor Test Plan
6. ND Filter: OD 3.0 VIS, 12.5mm Dia. Non-Reflective ND Filter

1.3 Abbreviations and Acronyms

ADCS	Attitude Determination and Control System
DSS	Digital Sun Sensor
FOV	Field of View
MCU	MicroController Unit
ND-Filter	Neutral Density Filter
LPM	Low-Power Mode
SEM	Scanning Electron Microscope

2 Sensor Design

The digital sun sensor is based upon the Hamatsu S9132 Profile sensor. This is a CMOS based area sensor, which works with 8bit or 10bit logic (user configurable). In this board, the sensor is configured to use 8bit logic. This can however be changed at a later date with a hardware change to the PCB.

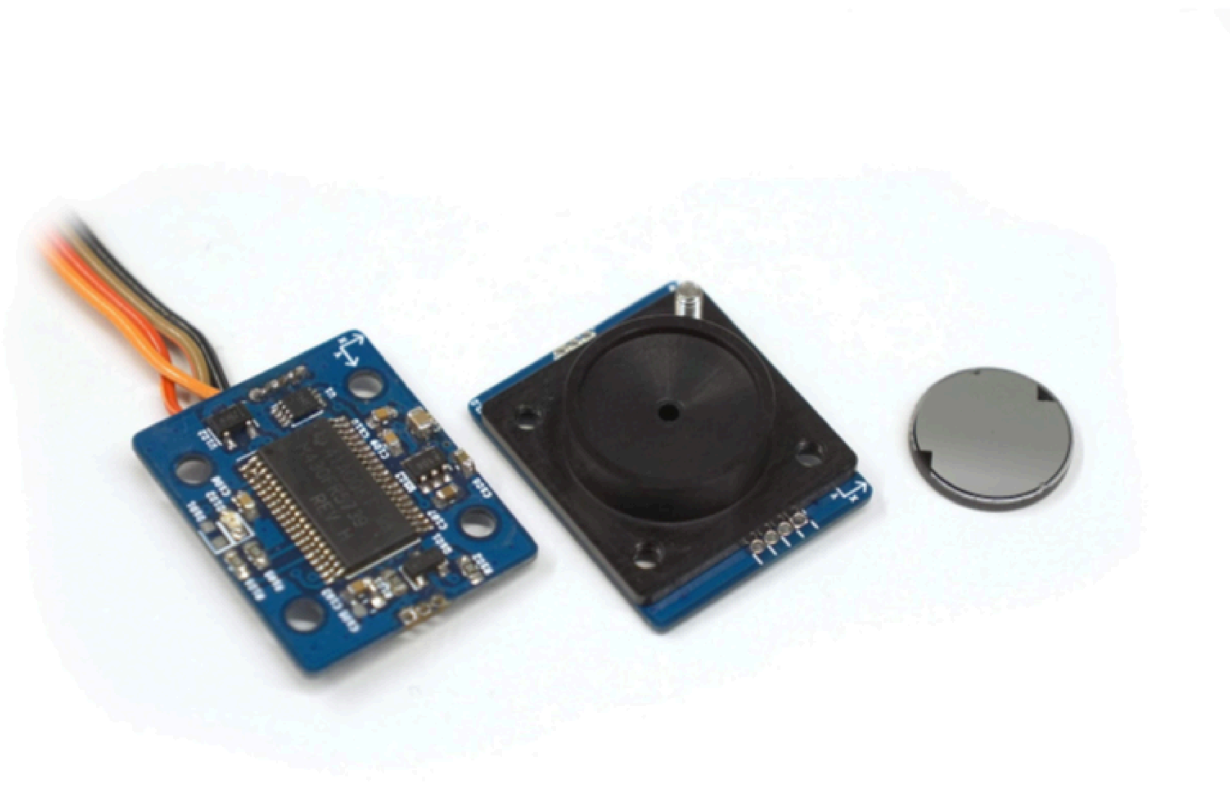

Figure 1. DSS PCB

The PCB of the DSS board consists of the front side, with the profile sensor, as well as the back side with the MSP430, power circuitry, RS485 transceiver and connectors to external power and programming.

The PCB design also incorporates 4×M2 mounting holes which connect the board to the cover and the hull of the satellite.

2.1 DSS General Characteristics:

- Dimensions: 20.4 × 24.8 × 7.0 mm
- Power consumption:
  - In use: ≈100 mW
  - Standby: ≈5 mW
- FOV: ≈50 degrees (Theoretical)
- Accuracy: ±0.1° (Theoretical)
- Boot up time: ≈500 ms

- Sampling time: ≈26 ms
- Operating voltage: 3–5 V:
    - 5 V charge-pump regulator
    - 3.3V LDO
- Serial Communication Interface: RS485
- ND-filter - 0.1 Transmission (%)
- Mask made with optical lithography
- 0.1 mm pinhole

2.2 Mechanical Cover

The DSS has an aluminum cover designed with Fusion 360. This mechanical cover provides protection to the S9132 sensor, as well as houses the ND-filter and mask inside. The cover will be made of space grade aluminum, which is anodized black.

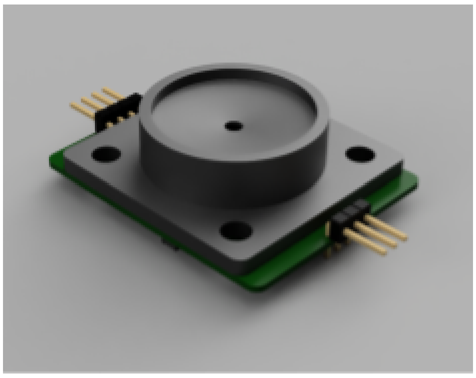

Figure 3. DSS Cover v4

The mask of the DSS is put on top of the ND-filter. The DSS cover has been designed with minimal tolerances, so that there is little to none excess space for the ND filter to move around. However, the tolerances in the design assume the worst case scenario for the dimensions of the ND-filter and S9132 profile sensor.

To ensure that the ND-filter and mask stays in one spot, the ND-filter will be glued to the aluminum cover using two part space grade epoxy glue. It is important to perform all the testing procedures defined in the FS1 ADCS Digital Sun Sensor Prototype Test Plan document after this, to ensure the correct calibration values and proper operation of the sensor.

For the manufacturing of the mechanical structure and the PCB of the sun sensor be sure to take a look at the FS1 ADCS Digital Sun Sensor Manufacturing Guide.

2.3 ND-Filter & Mask Design

The S9132 requires an ND-filter to reduce the intensity of the light hitting the surface of the sensor, otherwise the sensor will saturate and output values of maximum intensity. This results in loss of accuracy, once the center point of the light hitting the surface of the sensor is estimated.

The sensor must be able to withstand the intensity of light in the visual spectrum (to which it is most sensitive) while operating in space. The calculated ND-filter transmittance value should be around 0.1, in order to prevent saturation.

This is done with an Edmund Optics OD 3.0 VIS, 12.5mm Dia. Non-Reflective ND Filter, with a transmittance value of 0.1. The transmittance value is guaranteed to be within a tolerance of ±0.05% by the manufacturer. This value will also be verified during the EQM and flight model testing and characterization.

The mask design is a simple pinhole in the middle of the ND-filter with a hole of a diameter of 0.1 mm as shown in Figure 4. This shows an incoming incident light hitting the profile sensor surface. The ND-filter also provides additional UV-protection to the profile sensor.

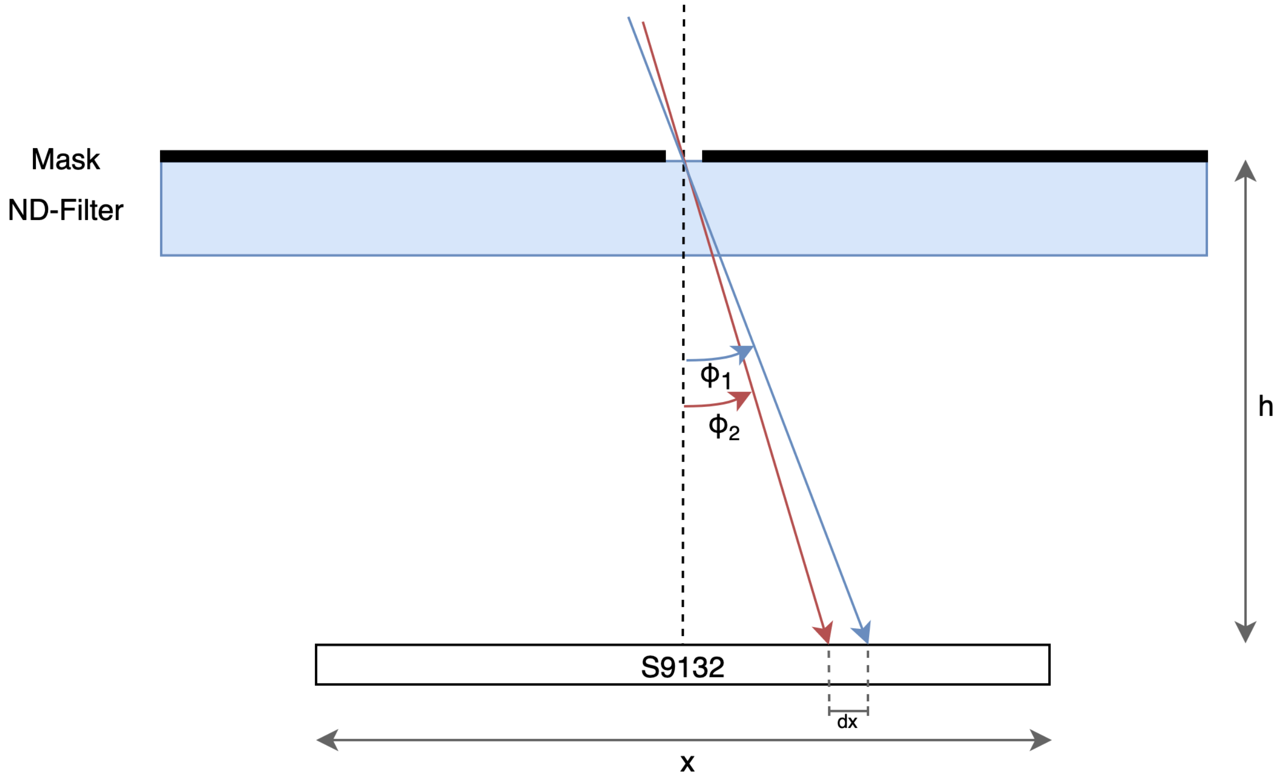

Figure 4. ND-filter & Mask

The film, which is set on top of the ND-filter, will have a titanium coating laid directly onto the glass surface with optical lithography. The titanium adheres strongly onto the glass layer, providing a strong bond. After this, an additional layer of aluminium will also be set on top of the layer of titanium, in order to provide better resistance to physical damage from sunlight and other sources. The aluminium also adheres better to a titanium surface compared to glass directly.

The diameter of the pinhole can be seen in Figure 5. This is an image taken with a SEM.

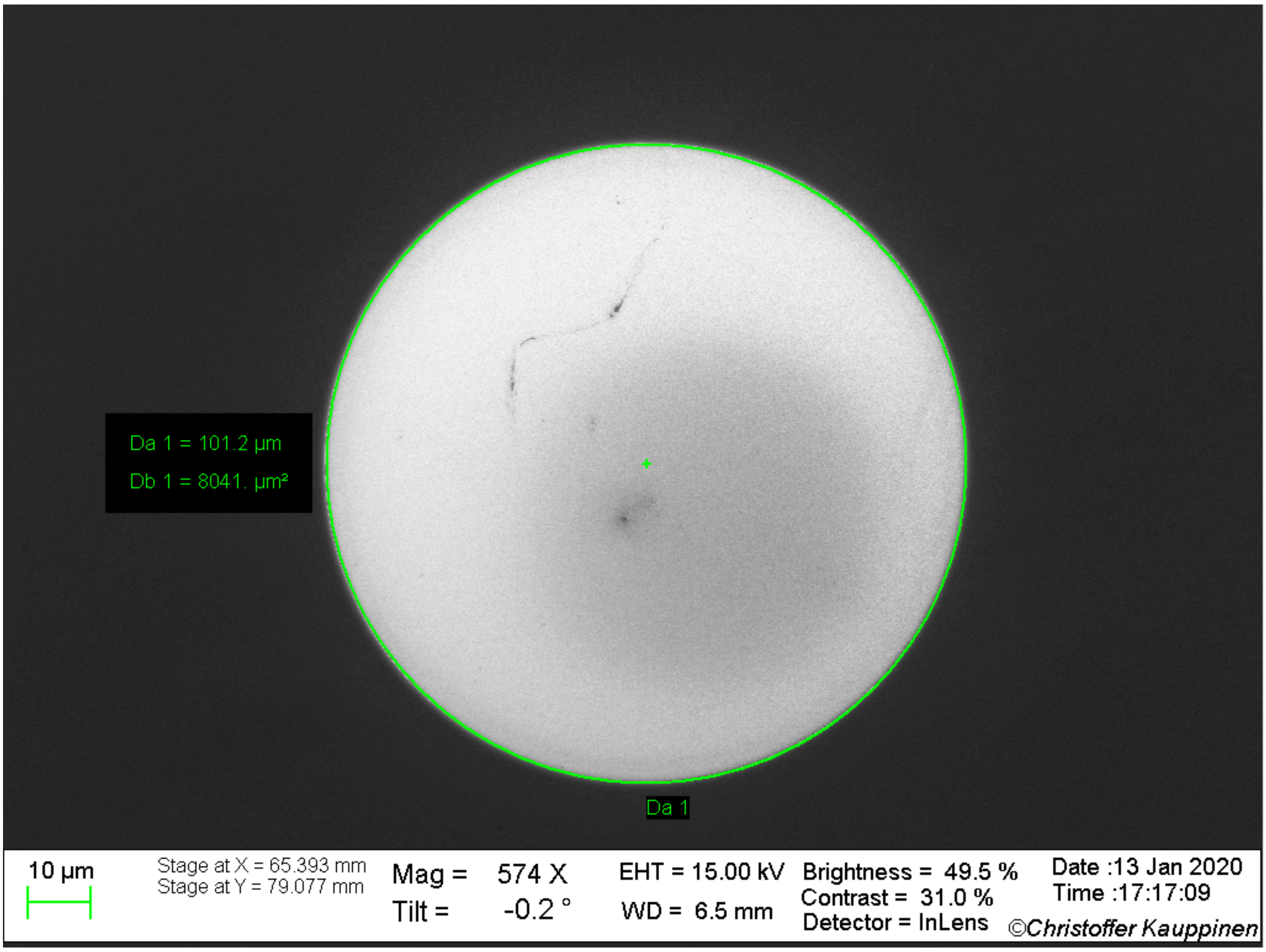

Figure 5. SEM picture of the pinhole

2.4 Theoretical FOV

The field of view (FOV) of a sun sensor is an integral part of its design, and a defining quality of the sensor. Different satellite designs have different requirements that the sun sensors must achieve. There is always a trade-off between the maximum theoretical accuracy and the FOV of a sun sensor.

The selection of the FOV of a sun sensor should be made in conjunction with the selection of the desired accuracy of the sensor. In addition to the theoretical analysis for these properties, one should also take into account the practical limitations of the hardware on the sensor.

The FOV of a pinhole-based sun sensor is affected by the height of the mask from the sensor's surface, the location of the pinhole relative to the center spot of the sensor and the physical constraints of the enclosure. The equation governing the maximum theoretical FOV of a sun sensor is:

$$\phi_{FOV} = 2tan^{-1}(\frac{x}{2h})$$

, where h is the height of the pinhole from the sensor surface and x array length of the sensor.

2.5 Theoretical accuracy

The accuracy of a sun sensor is not a property that should be addressed alone, as the FOV impacts the theoretical accuracy and vice versa. A higher pinhole height leads to a better accuracy, as the FOV is limited. This is because the sensor has a finite amount of pixels, which are used for measurements. So a smaller FOV in theory equates to a better accuracy as the sensor can utilise more pixels to distinguish a variation of one degree.

The linear resolution x is the distance in m between the individual pixels on the profile sensor. The accuracy of a sun sensor can be derived from the pinhole height and the linear resolution of the sensor. Referring to Figure 4, the accuracy is the difference between ϕ_1 and ϕ_2, when dx is equal to the linear resolution. This gives us the following relation for the maximum theoretical accuracy:

$$\phi_{Accuracy} = |\phi_1 - \phi_2|$$
$$\phi_{Accuracy} = |tan^{-1}(\frac{x}{h}) - tan^{-1}(\frac{x + dx}{h})|$$

The equation, which relates the FOV and the accuracy of a sun sensor is:

$$\phi_{FOV} = 2tan^{-1}(\frac{d}{2}\frac{\phi_{Accuracy}}{x})$$

, where d is the array size and x is the linear resolution.

3 Electrical Design

The electrical design of the sun sensor has been done in KiCad 5.0. Key design objectives have been a reduced power consumption, and the reliable operation of the sensor board.

3.1 Microcontroller

The DSS has a Texas Instruments MSP430FR5739 microcontroller embedded into its design, operated at 24 MHz, which handles data processing and interfacing with the rest of the ADCS on-board the OBC.

If needed, the MCU can also be operated at a lower frequency to reduce power consumption.

MCU characteristics:

- 16-Bit RISC Architecture up to 24-MHz Clock
- –40°C to +85°C Operation
- 16 KB of Nonvolatile FRAM Memory
- RS485 communication protocol
- 2.0 V to 3.6 V operating voltage

The MCU also has an integrated watch-dog timer (WDT), which ensures that the MCU is rebooted if it detects a halt in the main loop if code execution lingers for longer than a certain time period. The WDT will be used to prevent a situation, where the sensor becomes unresponsive, due to a fault in the MCU.

This WDT has not yet been implemented on the DSS.

3.2 S9132 Profile Sensor

The S9132 profile sensor is a CMOS area sensor, which provides 8-bit data to the MCU. This data is provided in the form of two histograms, which each contain the profile sensor data from the x- and y-axis.

The profile sensor spectral response can be seen in Figure 6. The spectral response shows that the sensor is most sensitive to light in the visible spectrum (≈500–700nm).

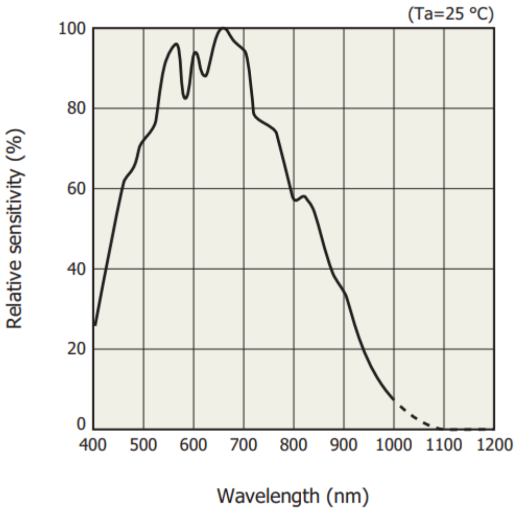

Figure 6. S9132 Spectral Response

The S9132 profile sensor can be used with a frequency up to 10 MHz in 8-bit mode, with a rated power usage of 75 mW. The analog supply voltage of the sensor must be ≈5 V, while the digital logic side supply voltage can vary between 3-5 V. The digital supply voltage is supplied from the same LDO circuit on the board. This is to ensure the same digital signal levels for the sensor and MCU, so that they can communicate with each other as the MCU is not 5 V tolerant.

3.3 Power Supply

For power, the board has a boost DC/DC charge-pump converter, which transforms the incoming 3.6 V satellite bus voltage into the 5 V needed by the S9132 profile sensor. A low-dropout regulator (LDO) provides the 3.3 V power input for the MCU. This is also directly converted down from the bus voltage.

Additionally bypass capacitors are set to reduce ripple in the 5 V power line. With a 10 uF 0805 bypass capacitor on the output of the charge-pump, it is possible to reduce the largest deviation in voltage down to 39m V @5 V (from around 100 mV).

Figure 7. 5V Line Ripple

The rise time of the 5V line on the DSS is around 350 µs as seen in the figure below. This time must pass before usage of the profile sensor can start. This is to ensure that the power level is stable during the operation of the sensor, and that the sensor produces accurate and reliable data.

Figure 8. 5V Line Rise Time

3.4 Inrush current

Inrush current of the DSS was measured using an external LTC4368 circuit, which is also used in other subsystems of the satellite. The DSS is capable of shutting down and powering back up the profile sensor in an effort to reduce power consumption while not in use. However, due to the high capacitance of the boost regulator output line, there is a large inrush current while powering up the profile sensor. The figure below shows the inrush current of the device, while applying a voltage of 3.6V.

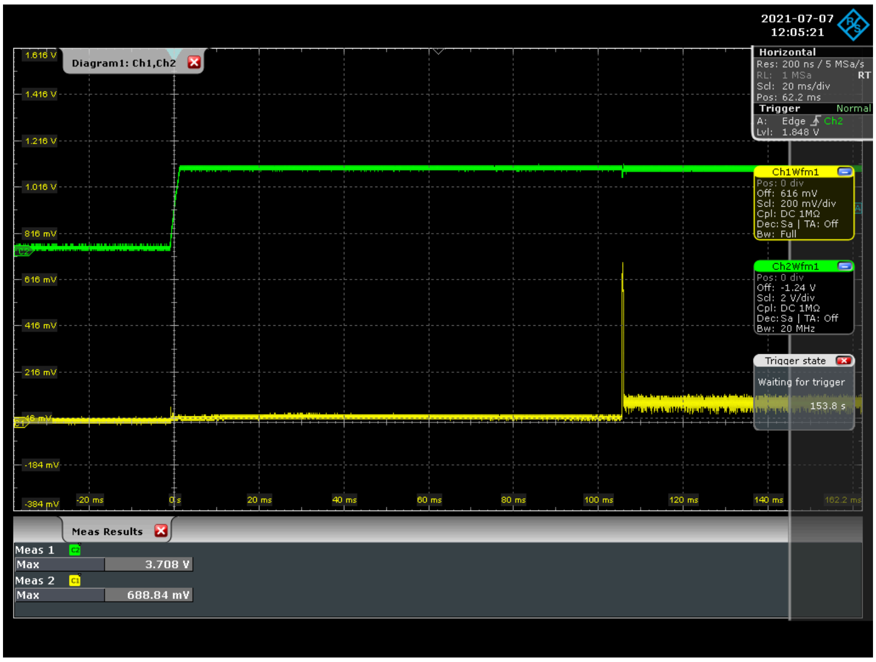

Figure . DSS Inrush current

The DSS was set up to wait for approximately 100ms prior to enabling the boost converter, which runs the profile sensor. From the Figure above it can be seen that the maximum voltage of the current sense line was 689mV, which equates to an inrush current of approximately **276mA** when the boost converter is enabled.

Needless to say the inrush current of the DSS is far too high for the system with the current configuration. The output capacitance of the boost converter output line is 10uF, which is most likely the source of this spike in current consumption. Action should be taken to mitigate and limit the effects of this behavior.

Unfortunately reducing the capacitance of the output line will increase the output voltage ripple, as discussed in the previous subsection. Thus, in order to fix the issue, a different boost converter is needed, or the system must be configured to provide the current necessary to overcome this inrush current.

The Voltage/Inrush current relationship was also examined for the 5V line on the DSS. The result can be seen from the Figure below.

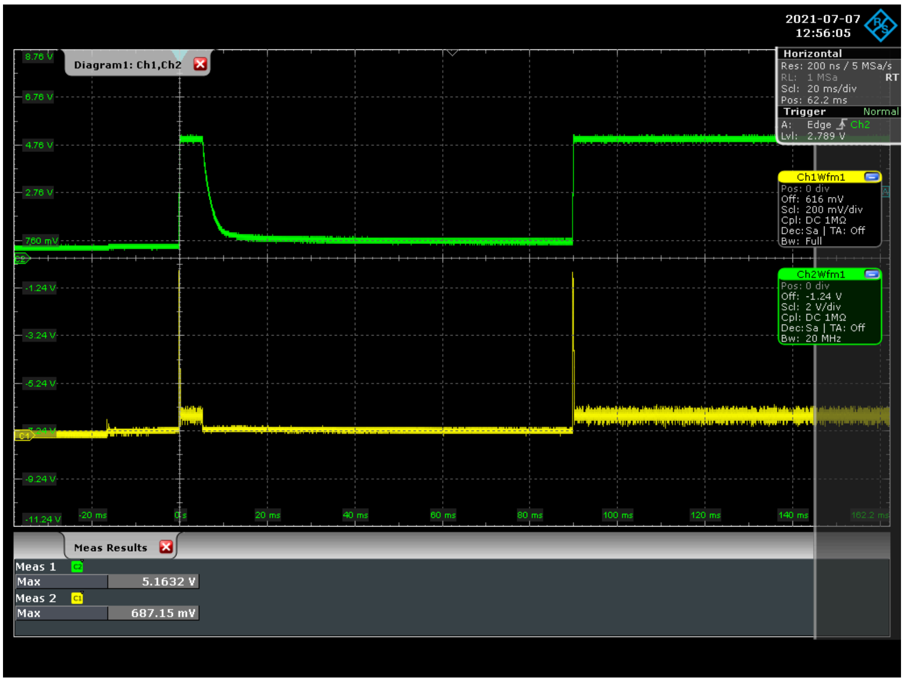

Figure . 5V Inrush current

During initial start-up, the MSP430 does not pull down the boost enable pin, which results in an inrush current spike during power-on. **To prevent this unwanted behavior, a pulldown resistor should be added on the boost enable line.**

Examining the inrush current of the 5V line a little closer, we can determine the ramp rate of the voltage line and the inrush current during this stage. The 5V line in comparison to the current consumption can be seen from the Figure below.

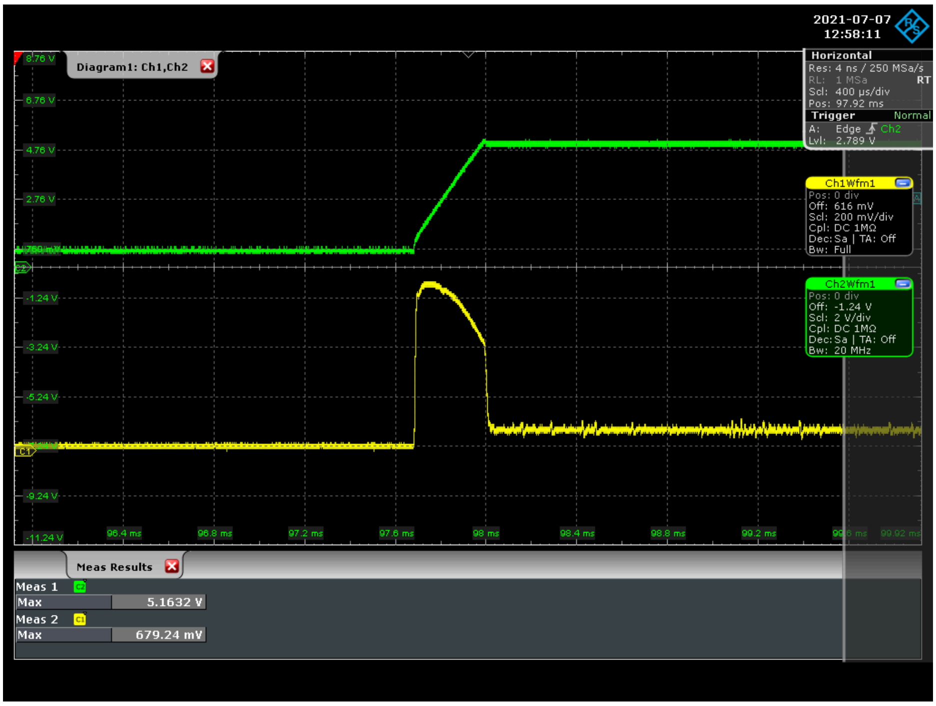

Figure . 5V Ramp-up

As can be seen from the Figure above, the inrush current spikes immediately after voltage is applied to the line and starts decreasing, while the voltage ramps up. This suggests that we are able to limit the inrush current by slowing down the ramp-up rate of the 5V line. This can be accomplished with an external MOSFET circuit.

3.5 Sensor Gain Selection

The S9132 has a controllable hardware sensor gain setting for both x- and y-axes. The gain affects the sensor's sensitivity to light. A 5V digital signal line is required to control the gain on the S9132, this command is provided by the MCU on the board.

The MSP430 however is not 5 V tolerant and thus is not capable of providing the needed voltage. To solve this, the gain setting is controlled by the MCU via an N-channel MOSFET, which drives the voltage on the gain pin from a logical high to a logical low through a pull-up resistor.

3.6 Environment

The table shows the maximum recommended operating temperatures specified by the manufacturers of the components.

Table 1. Environment Characteristics

Part	Recommended Operating Temperature Range
Hamamatsu S9132 Profile Sensor	−5°C to +65°C
MSP430FR5739 Microcontroller	−40°C to +85°C
TLV733P-3.3V	−40°C to +150°C
THVD14xx	−40°C to 125°C

4 Software

The software design of the Digital Sun Sensor is documented in the FS1p ADCS Digital Sun Sensor Software Design. This includes the overall architecture, algorithms and interfacing guide.

5 Calibration and Validation

The calibration and validation of the digital sun sensor is documented in the FS1 ADCS Digital Sun Sensor Prototype Test Plan document.

Tests and calibrations are performed with python scripts. A host Windows computer is used to communicate with the DSS through a FTDI RS485 cable. The scripts that run calibration and testing of the DSS can be found on the Github repository at the following location:
https://github.com/aaltosatellite/fs1p_adcs/tree/main/testing_scripts

Additionally the unit test system can be used to perform a basic functional test after manufacturing.
https://github.com/aaltosatellite/fs1p_tests/blob/main/egse_tests/test_sunsensor.py

Appendices

PCB Layout

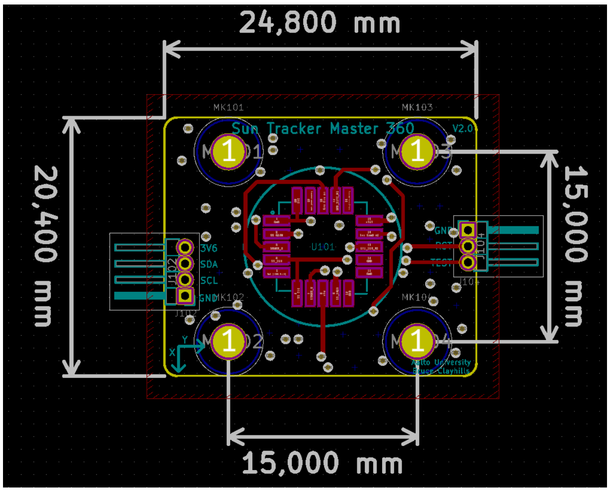

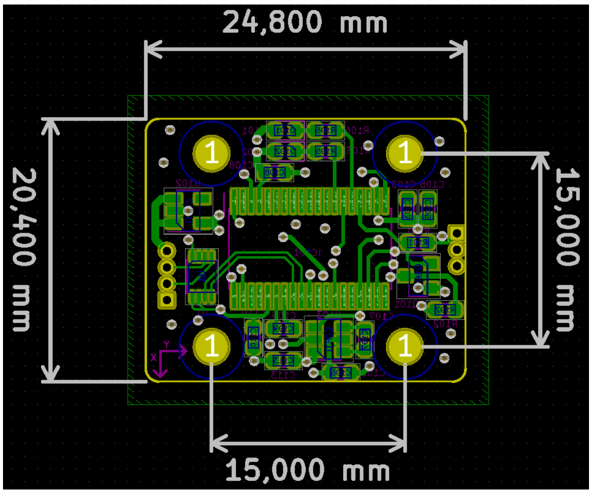

Dimensions:	24.80 x 20.40 mm
Mounting Hole Spacing:	15 mm
PCB Thickness:	0.8 mm